Article

Chemical reactivity of emodin and its oxidative metabolites to thiols

Boyang Qin, Yang Xu, Jiaming Chen, Wenlin Huang, Ying Peng, and Jiang Zheng

Chem. Res. Toxicol., **Just Accepted Manuscript** • DOI: 10.1021/acs.chemrestox.6b00191 • Publication Date (Web): 16 Nov 2016

Chemical reactivity of emodin and its oxidative metabolites to thiols

Boyang Qin,[†] Yang Xu,[§] Jiaming Chen,[†] Wenlin Huang,[θ] Ying Peng,[†]* and Jiang Zheng[‡¶]*

[†]School of Pharmacy, [§]School of Traditional Chinese Medicine, [‡]Key Laboratory of Structure-Based Drug Design & Discovery of Ministry of Education, Shenyang Pharmaceutical University, Shenyang, Liaoning, 110016, P. R. China

[θ]Department of Biochemistry, University of Washington, Seattle, WA 98195, USA

[¶]Key Laboratory of Pharmaceutics of Guizhou Province, Guizhou Medical University, Guiyang, Guizhou, 550004, P. R. China

Running title:

Bioactivation of emodin

Corresponding Authors:

Jiang Zheng, PhD
Key Laboratory of Structure-Based Drug Design & Discovery of Ministry of Education, Shenyang Pharmaceutical University, Shenyang, Liaoning, 110016, P. R. China
Key Laboratory of Pharmaceutics of Guizhou Province, Guizhou Medical University, Guiyang, Guizhou, 550004, P. R. China
Email: zhengneu@yahoo.com
Tel: 206-884-7651; Fax: 206-987-7660

Ying Peng, PhD
School of Pharmacy, Shenyang Pharmaceutical University, PO Box 21,103 Wenhua Road, Shenyang 110016, P. R. China
Email: yingpeng1999@163.com
Tel: +86-24-23986361; Fax: +86-24-23986510

TOC Graphic

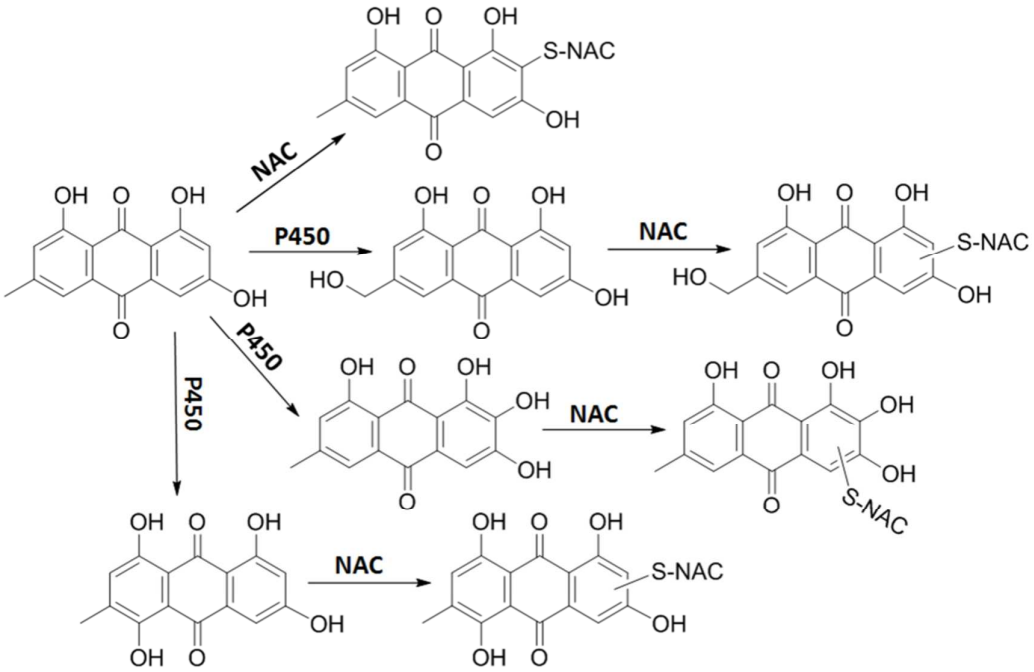

ABSTRACT

Polygonum multiflorum is a herbal medicine widely employed in China. Hepatotoxicity of the herbal medicine has been well documented, but the mechanisms of the toxicity remain unknown. Emodin (EM) is a major constituent of the herb and has been reported to be hepatotoxic. The main purposes of this study were to define the metabolic pathways of EM to characterize the potential reactive intermediates. EM was incubated with rat liver microsomes or human liver microsomes, followed by LC-MS/MS analysis to investigate the in *vitro* and in *vivo* metabolism of EM. As a result, three mono-hydroxylation metabolites (M1-M3) were detected after exposure to EM. The three metabolites were ω-hydroxyemodin, 2-hydroxyemodin, and 5-hydroxyemodin. Urinary M1 and M2 were detected in rats administered EM. Three mercapturic acids (M4–M6) were found in microsomal incubations containing EM, NADPH, and *N*-acetyl cysteine. It appears that M4 originated from parent compound EM, and M5 and M6 originated from M1 and M2, respectively. Two biliary EM-derived GSH conjugates were found in EM-treated rats. One arose from direct adduction of EM with GSH, and the other was derived from M1. P450s 1A2, 2C19 and 3A4 were the predominant P450 enzymes to oxidize EM. The findings assisted us to understand the mechanisms of EM-induced hepatotoxicity.

INTRODUCTION

Polygonum multiflorum, Heshouwu in Chinese, is a popular herbal medicine and functional food widely consumed in China and some Asian nations, due to reported tonic and anti-aging effects. The herbal medicine has officially been listed in Chinese Pharmacopeia.[1,2] The herb has been found to possess hair-blacking. Recent studies demonstrated that it exhibited antioxidative activity in mice and rats.[3-6] The chemical components found in polygonum multiflorum include anthraquinones, stilbene glucosides and phospholipids. Emodin (EM, Scheme 1) is the major one among the anthraquinone compounds. EM has been found to elicit antipyretic and anti-inflammatory properties.[7,8] Both extracts of polygonum multiflorum and purified EM showed inhibitory effects on receptor tyrosine kinase activity and tumor cell growth, along with antibiotic, anti-viral, and cytostatic activities.[9] Despite this, numbers of hepatic toxicity cases associated with polygonum multiflorum have been documented.[10-12] Additionally, EM was a primary component reportedly responsible for polygonum multiflorum induced hepatotoxicity. Cytotoxicity was also observed in L-02 and BEL cells after exposure to EM at concentration of 50 μM.[13]

Phase I metabolism studies demonstrated that EM was biotransformed to several hydroxylation metabolites in liver microsomes obtained from varieties of animal species. The oxidative metabolites were most likely 2-, 4-, 5-, and 7-hydroxyemodin as well as ω-hydroxyemodin. The structure of 2-hydroxyemodin was confirmed by mass spectrometry and NMR.[14-16] 2-Hydroxyemodin and ω-hydroxyemodin were reportedly genotoxic.[17]

The reported oxidative metabolism and toxicity of EM encouraged us to investigate metabolic activation of EM. The aims of the present work included (1) determination of the electrophilicity of EM; (2) characterization of reactive intermediates of EM in liver microsomes and in rats; (3) elucidation of the pathways of the metabolic activation of EM; and (4) identification of cytochromes P450 enzymes associated with EM bioactivation.

EXPERIMENTAL PROCEDURES

Chemicals and Materials

EM with purity of >98% was purchased from Chengdu Pufeide Biologic Technology Co., Ltd. (Chengdu, China). Glutathione (GSH), NADPH, and *N*-acetyl cysteine (NAC) were obtained from Sigma-Aldrich Co. (St. Louis, MO). Recombinant human P450 enzymes and human liver microsomes were from BD Gentest (Woburn, MA). Rat liver microsomes were prepared from Sprague-Dawley rats (male), based on the procedure we published earlier.[18] Diazepam was provided by the National Institute for the Control of Pharmaceutical and Biologic Products (Shenyang, China). Distilled water was from Wahaha Co., Ltd. (Hangzhou, China). All organic solvents were from Fisher Scientific (Springfield, NJ). All reagents and solvents were of either analytical or LC grade.

Animal Experiments

The treatment of rats followed the requirements of the Ethics Review Committee for Animal Experimentation of Shenyang Pharmaceutical University. Sprague-Dawley rats (200 ± 20 g, male) were provided by the Animal Center of Shenyang Pharmaceutical University (Shenyang, China). Animals were maintained in a temperature-controlled (22 ± 4 °C) room with a 12 h dark/light cycle and kept on standard rat chow. Rats were randomly divided into two groups, and each group contained 3 rats. Each rat was individually placed in a metabolism cage. Control samples contained the urine collected from rats after an overnight fast with free access to water before the treatment. Rats were given intraperitoneally with EM (50 mg/kg) dissolved in corn oil. The resulting 0-24 h urine was collected after

administration. During the experiments, the animals had free access to food and water. The other group of rats were fasted overnight but provided with free access to water and were treated with chloral hydrate to be anesthetized. Their bile ducts were cannulated using PE-10 tubing. Blank bile was collected prior to i.p. administration with EM at 50 mg/kg, and 0-24 h bile was collected postdose.

Sample Preparation for LC-MS/MS Analysis

The resulting urine or bile samples (100 μL) was mixed with acetonitrile (300 μL), followed by vortexing and centrifugation. The supernatants were collected and concentrated under nitrogen flow at 40 °C. The resulting concentrates were reconstituted with 50% acetonitrile in water (100 μL) and centrifuged at 19,000 *g* for 10 min. The resultant supernatants (5 μL) were subjected to LC-MS/MS analysis.

Microsomal Incubations

EM was dissolved in dimethyl sulfoxide (DMSO) as stock solution. The incubation system consisted of human or rat liver microsomes (1.0 mg protein/mL), 10 mM NAC or 10 mM GSH, 3.2 mM $MgCl_2$, and 50 μM EM in 300 μL potassium phosphate buffer (pH=7.4). The reactions were launched by addition of NADPH (1.0 mM). The control group lacked NADPH. The reactions were terminated by mixing with ice-cold acetonitrile (1:1 v/v) after 30 min incubation at 37 °C. The reaction mixture was vortex-mixed, followed by centrifugation at 19,000 *g* for 10 minutes at 4 °C. The supernatants were collected and concentrated to dryness under nitrogen flow and re-dissolved in 50% acetonitrile in water (100 μL). A 5 μL aliquot of the reconstituted solution was subjected to LC-MS/MS analysis. Each incubation was conducted in duplicate. In another study, the microsomal reactions were conducted

under similar condition without NAC or GSH.

Determination of air-labile reactions

The incubation mixture contained rat liver microsomes (1.0 mg protein/mL), NAC (10 mM), EM (50 μM), and $MgCl_2$ (3.2 mM) in potassium phosphate buffer (final volume: 300 μL). The incubation system was purged with nitrogen, and the reactions were started by mixing with NADPH (1.0 mM). The control microsomal incubations were performed under the same condition except the absence of NADPH. The reactions were terminated by addition of ice-cold acetonitrile (1:1 in volume) under nitrogen after 30 min incubation at 37 °C, followed by vortex-mixing and centrifugation at 19,000 *g* for 10 minutes at 4 °C under nitrogen. A 5 μL aliqot of the supernatants was subjected to LC-MS/MS analysis. The rest of sample was vortexed in the air for 20 min and resubmitted to LC-MS/MS for further analysis. In another study, EM (200 μM) and NAC (40 mM) were mixed in a final volume of 200 μL potassium phosphate buffer (pH 7.4) with 30 min incubation under nitrogen at 37 °C. The resulting mixture (5 μL) was submitted to LC-MS/MS for analysis. A part of the mixture was vortexed in the air for 20 min and resubmitted to LC-MS/MS analysis.

Chemical Synthesis of EM Metabolites

2-, 4-, and 7-hydroxyemodin (Scheme 1) were chemically synthesized from EM, according to a published protocol.[19] Briefly, potassium persulfate (52 mg) was dissolved in an EM-containing (20 mg) sulfuric acid solution (1 mL). The resulting mixture was stirred for 15 min at room temperature, and a further quantity of potassium persulfate (52 mg) added with additional 50 min stirring. The resultant violet solution was diluted with water (20 mL). The resulting orange suspension was

mixed with sodium metabisulfite (200 mg), followed by extraction with ethyl acetate (3 mL). After evaporation of the organic solvent, the residues were reconstituted with the initial mobile solvent and submitted to an LC-MS/MS system. Desired product 2-hydroxyemodin was purified by silica gel chromatography and characterized by mass spectrometry and NMR. ^{1}H-NMR (CD_3OD, 600 MHz): δ2.17 (3H, s, C-11), 6.20 (1H, s, H-4), 6.82 (1H, d, *J*=2.0 Hz, H-7), 6.90 (1H, s, H-5).

5-Hydroxyemodin (Scheme 1) was synthesized by oxidation of EM with boric acid.[19] To a solution (1 mL) of boric acid (50 mg) in 65% oleum was EM (10 mg) added, and the flask was sealed. The mixture was stirred at room temperature for 5 h and poured onto ice (25 g), followed by boiling for 10 min and cooling to room temperature. The resulting precipitates were reconstituted in a KOH solution (0.2 M, 20 mL) purged with nitrogen. The resultant solution was heated at 100 °C for 15 min, acidified with 5% HCl, and extracted with ethyl acetate (5 mL). The organic phase was washed with H_2O (3 x 5 mL) and concentrated by rotary evaporation. The product was recrystallized from dilute acetic acid and submitted to LC-MS/MS analysis.

ω-Hydroxyemodin (Scheme 1) was prepared by the oxidation of the methyl moiety of EM.[20] To an EM (20 mg) solution in acetic acid were acetic anhydride (1 mL) and concentrated sulfuric acid (10 μL) added slowly. The resulting mixture was stirred at 70 °C for 30 min and poured to ice water to afford crystals of 1,3,8-triacetylemodin (TAEM). An acetic acid solution (50 mL) containing chromium (VI) oxide (CrO_3, 600 mg) was dropwise added to a solution of TAEM (25 mg) dissolved in a mixture of glacial acetic acid (1 mL) and acetic anhydride (1 mL). The resulting mixture was stirred at room temperature for 24 h to produce 1,3,8-triacetylemodic

acid (TAEA) as crystals. TAEA (5 mg) was dissolved in 500 μL dry tetrahydrofuran, followed by addition of boron-methyl sulfide complex (175 μL) in tetrahydrofuran precooled at 0 °C. After 1 h stirring at 0 °C, the reaction was quenched by mixing with water (1 mL). The resulting aqueous solution was extracted with ethyl acetate. The unreacted TAEA was washed off using 5% $NaHCO_3$ aqueous solution. The reaction gave 1,3,8-triacetyl-ω-hydroxyemodin (TA-ω-OHEM). ω-Hydroxyemodin was obtained through hydrolysis of TA-ω-OHEM in a potassium hydroxide solution with stirring at 75 °C for 15 min. The resultant mixture was acidified, and ω-hydroxyemodin was extracted with ethyl acetate and recrystallized from ethanol.

NAC conjugates, such as M4, M5, and M6, were synthesized by direct reaction of NAC with the corresponding electrophilic agents. EM, ω-hydroxyemodin, and 2-hydroxyemodin were individually dissolved in potassium phosphate buffer and mixed with NAC, followed by 1 h stirring at 37 °C and centrifugation at 19,000 *g* for 5 min. The supernatants were analyzed by LC-MS/MS. The EM-derived NAC conjugate was purified by a semi-preparative HPLC system. The purified product was characterized by mass spectrometry and NMR. ^{1}H NMR (CD_3OD, 600 MHz): δ2.40 (3H, s, H-11), 6.08 (1H, s, H-4), 6.95 (1H, s, H-7), 7.46 (1H, d, *J*=0.9 Hz, H-5); ^{13}C NMR (CD_3OD, 600 MHz): δ20.54 (C-11), 104.91 (C-9a), 107.07 (C-4), 113.97 (C-8a), 119.08 (C-5), 122.10 (C-7), 129.48 (C-2), 134.95 (C-10a), 145.67 (C-6), 160.92 (C-8), 166.03 (C-3), 171.13 (C-1), 184.67 (C-10), 185.26 (C-9).

2-Hydroxyemodin, 5-hydroxyemodin, and ω-hydroxyemodin were individually dissolved in potassium phosphate buffer and mixed with GSH, followed by 60 min stirring at 37 °C and centrifugation at 19,000 *g* for 5 min. The supernatants were injected on to the LC-MS/MS for analysis.

Recombinant Human P450 Enzyme Incubations

Nine recombinant human P450 enzyme, including P450s 2A6, 1A2, 2C19, 2C9, 2B6, 2D6, 3A4, 2E1, and 3A5, were selected for the determination of the specific P450 participating in the formation of reactive metabolites of EM. Incubation mixtures contained 100 nM recombinant human P450 enzyme, 50 μM EM, 1 mM NADPH, and 10 mM NAC (final volume: 300 μL). After 30 min incubations at 37 °C, and reactions were quenched by addition of an equal volume of ice-cold acetonitrile containing diazepam as the internal standard (final concentration, 250 ng/mL). Each incubation was carried out in duplicate. The formation of EM metabolites was monitored by LC-MS/MS. The rates of metabolite production in individual incubations with the recombinant P450 enzymes were multiplied by the mean specific content of the corresponding P450 enzyme in human liver microsomes to obtain the normalized reaction rates of each enzyme.[21]

Determination of k_{cat} and K_m

To determine k_{cat} and K_m of P450s 2C19 and 1A2 for metabolism of EM, six different concentrations of EM were applied, including 10, 50, 100, 400, 1,600, and 2,400 μM. The concentration of the recombinant human P450 enzymes was 100 nM. The incubation mixtures also contained 1 mM NADPH and 10 mM NAC (final volume: 200 μL). After 10 min incubations at 37 °C, and reactions were quenched by addition of an equal volume of ice-cold acetonitrile containing diazepam as the internal standard (final concentration: 250 ng/mL). Incubations were conducted in triplicate. The production of M1 was monitored and quantitated by LC-MS/MS.

LC-MS/MS Method

Analyses were carried out on an AB SCIEX Instruments 4000 Q-Trap (Applied Biosystems, Foster City, CA) equipped with an ekspert ultraLC 100 system (Applied Biosystems, Foster City, CA). The separations of analytes were established on an Accuore C18 column (2.1×50 mm, 2.6 μm) (Thermo Fisher, Pittsburgh, PA). The flow rate was set at 0.8 mL/min. The mobile phases consisted of acetonitrile with 0.1 % formic acid (A) and 0.1 % formic acid in water (B) with a gradient elution of 10 % A at 0−2 min; 10−95 % A at 2−12 min; 95−95 % A at 12−17 min; 95−10 % A at 17−18 min; and 10−10 % A at 18−20 min. A 5 μL aliquot of samples was applied on LC-MS/MS for analysis. The samples were analyzed in positive-ion mode. The mass spectrometer was operated with a turbo ion spray by use of conditions as follow: ion spray voltage, 5500 V; source temperature, 650 °C; curtain gas, 20 psi; ion source gas 1, 50 psi; ion source gas 2, 50 psi; entrance potential, 10 V; and cell exit potential, 3 V. Thereafter, optimization of MS/MS conditions was performed for the internal standard by infusing the individual solution into the Electrospray source. The parameters were optimized in MRM mode in order to achieve the highest sensitivity possible. As a result, the characteristics of ion pairs (corresponding to declustering potential DP, collision energy CE) were *m*/*z* 287→139 (100, 68) for hydroxylation metabolites, *m*/*z* 576→327 (100, 40) and, 592→463 (100, 40) for GSH conjugates, *m*/*z* 432→301 (100, 40) and, 448→317 (100, 40) for NAC conjugates, and *m*/*z* 285→193 (70, 50) for diazepam (internal standard). The information-dependent acquisition (IDA) method was employed to trigger the enhanced product ion (EPI) scans by analyzing MRM. The EPI scan was run in positive mode at a scan range for product ions from *m/z* 50 to 300 or 100 to 500. The collision energy (CE) was set at 35 eV with a spread of 15 eV. Data were processed using Applied Biosystems/SCIEX

Analyst software (versions 1.6 and 1.6.1).

Synthetic products were purified on a YMC-Pack ODS-A column (250×10 mm, S-5, 12 nm) (YMC Co., Ltd, Japan), and the purification was achieved on a semi-preparative HPLC system. An isocratic elution was employed for the product purification with 45 % methanol in water. The low rate was 3 mL/min.

RESULTS

Mass Spectrometric Behaviors of EM

The fragmentation behaviors of the parent compound EM was determined to assist us to characterize the structures of EM metabolites. Analysis of EM was performed in positive ionization mode, which offered higher sensitivity and more fragment ions. The parent compound showed fragment ions of *m*/*z* 225 ($[MH\text{-}H_2O\text{-}CO]^+$), 197 ($[MH\text{-}H_2O\text{-}2CO]^+$), 169 ($[MH\text{-}H_2O\text{-}3CO]^+$), 141 ($[MH\text{-}H_2O\text{-}4CO]^+$), and 115 ($[MH\text{-}H_2O\text{-}4CO\text{-}C_2H_2]^+$), along with $[M+H]^+$ of *m*/*z* 271 (Figure 1), most likely resulting from a loss of CH_2O_2, $C_2H_2O_3$, $C_3H_2O_4$, $C_4H_2O_5$, and $C_6H_4O_5$, respectively.

Characterization of Oxidative Metabolites of EM

Three hydroxylation metabolites, namely M1-M3, were detected in both human and rat liver microsomes after exposure to EM (Figure 2A, S1A and S1D). However, the two metabolites with limited amounts were observed in the microsomal incubations where NADPH was excluded (Figure 2B). This indicates that P450 enzymes were involved in the formation of M1-M3. M1, M2, and M3, sharing the same molecular ions, were isomers of oxidative metabolites resulting from hydroxylation of EM at three different positions. Tandem mass spectra of M1-M3 were obtained through MRM-EPI scanning (transition ion *m*/*z* 287/139) (Figure 2F, 2G and 2H). The three metabolites exhibited characteristic fragment ions at *m*/*z* 213 ($[M+H\text{-}H_2O\text{-}2CO]^+$), 185 ($[M+H\text{-}H_2O\text{-}3CO]^+$), 157 ($[M+H\text{-}H_2O\text{-}4CO]^+$), 139 ($[M+H\text{-}2H_2O\text{-}4CO]^+$), and 128 ($[M+H\text{-}3H_2O\text{-}4CO]^+$). The observed product ions of *m*/*z* 213, 185, and 157 received mass gain of 16 Da relative to the corresponding ions at *m*/*z* 197, 169, and 141 found in the tandem mass spectrum of the parent compound (Figure 1).

This provided further evidence for the production of the hydroxylation metabolites of EM designated as M1-M3. A small amount of the hydroxylation metabolites were observed in the microsomal incubation where NADPH was excluded (Figure 2B), possibly due to the impurity resulting from auto-oxidation of EM.

Chemical oxidation of EM with persulfate in sulfuric acid produced three oxidative products, reportedly 2-, 4-, and 7-hydroxyemodin (Scheme 1).[19] One product showed the similar chromatographic and mass spectral properties as those of M2 (Figure 2D and 2J). The product was purified and characterized by NMR. The ^{1}H NMR spectrum showed three aromatic proton resonances at 6.20, 6.82, and 6.90 ppm responsible for the protons at C-4, C-7 and C-5, and methylic protons at 2.17 ppm corresponded to the protons at C-11. The obtained NMR spectrum of the product was similar as that reported for 2-hydroxyemodin.[17] ω-Hydroxyemodin (Scheme 1) was prepared by oxidation of EM using CrO_3.[20] The resulting hydroxylation product demonstrated the same chromatographic and mass spectrometric identities as those of M1 produced in microsomal incubations (Figure 2C and 2I). 5-Hydroxyemodin (Scheme 1) was synthesized by oxidation of EM with boric acid.[19] The LC-MS/MS analysis showed that 5-hydroxyemodin shared identical chromatographic and mass spectral behaviors as those of M3 (Figure 2E and 2K). Together, the synthetic work made us assign M1-M3 as ω-hydroxyemodin, 2-hydroxyemodin, and 5-hydroxyemodin, respectively.

Characterization of NAC conjugates

Three NAC conjugates (M4-M6) were observed in both human and rat liver microsomal incubations of EM fortified with NAC (Figure S1B, S1C, S1E and S1F). M4

with the retention time at 10.19 min (Figure 3A) had its $[M+H]^+$ ion at *m*/*z* 432, along with fingerprint product ions at *m*/*z* 303, 301, 162, 130, and 121 (Figure 3D). The product ion at *m*/*z* 130 corresponded to NAC moiety without the sulfur, and the fragment ion at *m*/*z* 162 was derived from NAC moiety with the sulfur. The product ion at *m*/*z* 303 corresponded to the characteristic neutral loss of 129 Da for the NAC conjugates.

M4 was detected in microsomal incubations in the absence of NADPH (Figure 3B). Direct reaction of EM with NAC in PBS buffer produced a product which revealed the same chromatographic and mass spectral behaviors (Figure 3C and 3E) as those of M4 produced in the microsomal incubations. The ^{1}H NMR, ^{13}C NMR and HMBC (long-range proton-carbon heteronuclear multiple bond correlation) spectrum data for M4 are shown in Figure 4. Five aromatic carbon signals at δC20.54 (δH 2.40, s), δC104.91, δC129.48, δC166.03, and δC184.67 were designated to C-11, C-9a, C-2, C-3, and C-10, respectively. The proton NMR spectrum presented three aromatic proton resonances at 7.46, 6.95, and 6.08 ppm, and the HMBC spectrum (Figure 4) showed that C-11 had correlations with the protons at 7.46 and 6.95 ppm, but no such correlation was observed between C-11 and the proton at 6.08 ppm. Thus, we tentatively considered that NAC was attached either at C-2 or at C-4 of EM. Additionally, the HMBC spectrum demonstrated that C-2, C-3, C-9a, and C-10 had correlations with the proton at 6.08 ppm. This made us conclude that NAC was connected to C-2 of EM (Scheme 2).

M5 and M6 monitored by MRM scanning with transition ion *m*/*z* 448→317 eluted out at 8.25 and 9.10 min respectively (Figure 5A and 6A). Only minor M5 and M6 were found in the incubation system without NADPH (Figure 5B and 6B). This

indicates that metabolic activation was involved in the generation of M5 and M6. The MS/MS spectra of M5 and M6 demonstrated the characteristic fragment ions responsible for the cleavage of the NAC moiety. The tandem spectrum of M5 provided product ions at *m*/*z* 121, 130, 162, 317, 319, and 406 (Figure 5D), and the tandem spectrum of M6 revealed fingerprint fragment ions at *m*/*z* 130, 162, 317, 319, 338, and 412 (Figure 6D). Product ion at *m*/*z* 319 corresponded to the characteristic neutral loss of 129 Da for the NAC conjugates resulting from the cleavage of the NAC moiety. The fragment ions of M5 and M6 at *m*/*z* 162 (loss of NAC moiety with sulfur) and 130 (loss of NAC moiety without sulfur) were found to be the same as those of M4. The molecular ions of M5 and M6 were found to be *m*/*z* 448 that is 16 Da more than the molecular ion of M4, and the observed fragment ions of M5 and M6 at *m*/*z* 319 and 317 were 16 Da more than the product ions of M4 at *m*/*z* 303 and 301. These results suggest that the formation of M5 and M6 resulted from hydroxylation of EM and then addition of a molecule of NAC.

To determine the origins of M5 and M6, synthetic M1 and M2 were individually mixed with NAC. The product obtained from M1-NAC reaction demonstrated the same chromatographic and mass spectral identities as those of M5 produced in microsomal incubations (Figure 5C and 5E). As expected, the product from M2-NAC reaction and M6 shared the same chromatographic and mass spectral behaviors (Figure 6C and 6E). Clearly, M5 and M6 originated from M1 and M2, respectively (Scheme 2).

Metabolic Activation of EM in Rats

In order to investigate the metabolic activation of EM in *vivo*, biliary and urinary

metabolites were monitored by MRM-EPI. Two oxidative metabolites were found in the urine of rats treated with EM (Figure 7A), and no such metabolites were observed in the urine before treatment (Figure 7B). The metabolites found in the in *vivo* studies showed the same chromatographic and mass spectral properties as those of M1 (ω-hydroxyemodin) and M2 (2-hydroxyemodin) formed in microsomal incubations or chemical synthesis (Figure 2, 7C and 7D).

Two metabolites (M7 and M8) with molecular ions of *m*/*z* 576 and 592 in the bile samples were detected. The observed molecular ions of *m*/*z* 576 and 592 matched the molecular weights of the GSH conjugate derived from EM and the GSH conjugate derived from hydroxylation metabolites of EM, respectively. We failed to detect such conjugates in the blank bile (data not shown). Metabolite M7 monitored by scanning of ion pairs at *m*/*z* 576→327 in positive ion mode was detected, and the metabolite eluted at retention time of 8.65 min (Figure 8A). The tandem spectrum of M7 demonstrated the major product ions associated with fragmentation resulting from the GSH moiety (Figure 8C). The primary fragment ions were *m*/*z* 327 and 430. Product ion *m*/*z* 430 resulted from the loss of the glutamine moiety (−146 Da) from *m*/*z* 576. The fragment ion at *m*/*z* 327 was derived from the loss of the *N*-formylglycine moiety (−103 Da) from *m*/*z* 430. In addition, the fragments at *m*/*z* 501 and 447 arose from the loss of the glycinyl moiety (−75 Da) and *γ*-glutamyl moiety (−129 Da) from *m*/*z* 576, respectively. Metabolite M8 (R_t = 9.18 min) was detected by monitoring of ion pair *m*/*z* 592→463 in positive ion mode (Figure 9A). The tandem mass spectrum of M8 also demonstrated the major fragments derived from fragmentation of the GSH moiety (Figure 9C). Primary fragment ion *m*/*z* 317 resulted from the loss of the glutathione moiety without the sulfur (−273 Da) and two

hydrogen atoms from *m*/*z* 592. The fragment ion at *m*/*z* 446 was derived from the loss of the glutamine moiety (−146 Da) from *m*/*z* 592. The fragment ion at *m*/*z* 343 was derived from the loss of the *N*-formylglycine moiety (−103 Da) from *m*/*z* 446. In addition, the fragment ion at *m*/*z* 463 was derived from the loss of the *γ*-glutamyl moiety (−129 Da) from *m*/*z* 592.

In a separate study, three GSH conjugates were observed in GSH-fortified rat liver microsomes after exposure to EM (Figure 8B and 9B). One of the conjugates demonstrated the same chromatographic and mass spectral properties as those of M7 (Figure 8A and 8C). Apparently, NADPH was unnecessarily required for the production of the conjugate (Figure 8B). Additionally, reaction of GSH with EM produced a product which revealed the same mass spectrum and retention time as M7. The other two GSH conjugates detected in the microsomal reaction demonstrated identical molecular ions (*m*/*z* 592). This suggests that the two were derived from hydroxylation metabolites of EM, based on their molecular ions and mass spectra observed (data not shown). One of the GSH conjugates showed the same retention time (R_t = 9.16 min) as that of M8 (Figure 9A). The incubation of GSH with synthetic M1 offered the GSH conjugate which showed the same chromatographic identities as that of M8 detected in the bile samples (Figure 9D, 9E and 9F). Obviously, M8 originated from M1.

P450 Enzymes Responsible for bioactivation of EM

Nine human recombinant P450 enzymes were individually incubated with EM fortified with NAC, and the formation of M1-M3 and M5-M6 was monitored to determine the specific P450 enzymes involved in the bioactivation of EM. P450 2C19

was found to be the major enzyme involved in the production of M1 and M5, and P450 1A2 was the primary enzyme participating in the generation of M2, M3, and M6. P450 3A4 catalyzed the formation of M1-M3 and M5-M6 of EM (Figure 10A and 10B). The results showed that the metabolism of EM was mediated by several P450 enzymes. In addition, the efficiencies of the P450s 2C19 and 1A2 were assessed by determining the values of k_{cat}/K_m (Table S1). The obtained results conformed to Michaelis-Menten equation, and reactions reached the saturated state when the concentration of the substrate were 1,600 μM for P450 2C19 and 1,600 μM for P450 1A2 (Figure S4), respectively. P450 2C19 (k_{cat}/K_m 0.0401) was found to be 14.9-fold more efficient than P450 1A2 (k_{cat}/K_m 0.0027), similar with the ratio observed in the one-concentration study (12.7-fold, Figure 10).

DISCUSSION

EM is a major component in Polygonum multiforum and is widely employed as a traditional Chinese medicine. The hepatotoxicity of polygonum multiflorum was reportedly associated with EM,[13] and the mechanisms of EM toxicity remain unknown. A comprehensive metabolism investigation was needed to better understand the mechanisms of EM toxic action. As an initial step for metabolite identification, the mass spectrometric behaviors and fragmentation patterns of EM were investigated (Figure 1). The LC-MS/MS analysis work facilitated the structural recognition of the EM moiety in the characterization of EM metabolites.

Three hydroxylation metabolites (M1-M3) were detected by a LC-MS/MS system in microsomal incubations of EM. A total of five hydroxylation metabolites are possibly generated, including 2-, 4-, 5-, and 7-hydroxyemodin arising from aromatic hydroxylation and ω-hydroxyemodin resulting from aliphatic hydroxylation (Scheme 1). Chemical synthesis was performed to characterize the three oxidative metabolites observed. Chemical oxidation of EM with persulfate offered three oxidative products, reportedly including 2-, 4-, and 7-hydroxyemodin.[19] One of the three showed the same retention time (10.75 min) and mass spectrum as that of M2. The NMR spectrum demonstrated that the product was 2-hydroxyemodin. Based on the chromatographic and mass spectrometric identities, M3 was characterized as 5-hydroxyemodin prepared by oxidation of EM with oleum and boric acid,[19] and M1 was assigned as ω-hydroxyemodin obtained by oxidizing of EM using CrO_3.[20] Mueller and coworkers reported two hydroxylation metabolites of EM, i.e. ω-hydroxyemodin and 2-hydroxyemodin.[17] In addition to the two hydroxylation metabolites, we detected 5-hydroxyemodin as a new oxidative metabolite of EM. The chemical

synthetic work led us to obtain five hydroxylation products of EM, but microsomal reaction offered only three, i.e. 2- and 5-hydroxyemodin as well as ω-hydroxyemodin.

Three NAC-derived conjugates (M4−M6) were found in microsomal incubations of EM supplemented with NAC. M4 was most likely formed by direct reaction of EM with NAC (Michael addition), followed by (spontaneous) oxidation. To probe the mechanism, we mixed EM with NAC in a buffer system. The reaction produced M4 with a high yield, indicating that the generation of M4 took place spontaneously. No hydroquinone **1** was detected in the reaction mixture. In a separate study, we mixed EM with NAC in a buffer system under nitrogen. Hydroquinone **1** (Scheme 2) was detected, but not M4. As expected, decreased hydroquinone **1**, along with the appearance of M4, was observed in the mixture after exposure to the air (Figure S3). This suggests that the hydroquinone is air-labile and was auto-oxidized to M4 instantly (Scheme 2).

M5 and M6 were apparently derived from hydroxylation metabolites of EM. The determination of origins of M5 and M6 were probed by reaction of NAC with the individual oxidative metabolites, i.e. M1-M3. M5 was found to originate from M1, and NAC conjugate M6 was derived from M2 (Scheme 2). Similar to the pathway for the formation of M4, M5 and M6 were likely generated by reaction of NAC with the corresponding hydroxylation metabolites, followed by auto-oxidation. In order to probe the hypothesis, we incubated EM with rat liver microsomes supplemented with NADPH and NAC under nitrogen. Hydroquinone **2** and **3** (Scheme 2) were detected, but neither M5 nor M6 was observed. Sequential exposure of the mixture to the air resulted in depletion of the two hydroquinone derivatives and production of M5 and M6 (Figure S3). Moreover, M6 could also be formed by oxidation of M2 to

ortho-quinone **4** which further reacted with NAC (Scheme 3). We were unable to detect the NAC conjugate generated from M3 in NAC-fortified microsomes after exposure to EM. However, direct reaction of NAC with synthetic M3 produced a product with similar mass spectrometric identities as that of M5 and M6 (Figure S2). The unsuccessfulness to observe the NAC conjugate derived from M3 possibly resulted from that the level of the conjugate was too low to be detected.

For *in vivo* EM metabolism study, bile and urine samples were collected from animals administered EM. M1 and M2 were detected in the urine, but we failed to detect such oxidative metabolites in the bile. As expected, the GSH conjugate directly adducted with EM was detected in the bile, providing the *in vivo* evidence for the reactivity of EM towards nucleophiles. Apparently, only one GSH conjugate (M8) derived from hydroxylation metabolites, specifically from M1, was detected in the bile. Interestingly, no mercapturates and other GSH conjugate-related conjugates derived from EM or/and its oxidative metabolites were observed in the urine. The failure to detect the urinary adducts remains unknown.

In summary, three hydroxylation metabolites were detected in EM-exposed rat and human liver microsomes, and they were 2-hydroxyemodin, 5-hydroxyemodin, and ω-hydroxyemodin. The oxidative metabolites, along with parent EM, were all found to be electrophilic species reactive to NAC and GSH. P450 1A2 and 2C19 were the primary enzymes mediating the bioactivation of EM. The findings allowed us to better understand the mechanisms of hepatotoxicity induced by EM.

Funding sources

This work was supported in part by the National Natural Science Foundation of China [Grant 81373471 and 81430086].

Supporting Information Available

Compare the difference between incubations in human and rat liver microsomes. Representative chromatographic trace and mass spectrometric identity for the NAC conjugate derived from 5-hydroxyemodin. Hydroquinone intermediates **1**-**3** were detected in the incubation of EM under nitrogen. The efficiencies of P450s 2C19 and 1A2 to oxidize EM were assessed by determining the values of K_m and k_{cat}. This material can be accessed via the Internet at http://pubs.acs.org.

Abbreviations

CE, collision energy; DMSO, dimethyl sulfoxide; DP, declustering potential; EM, emodin; EPI, enhanced product ion; GSH, glutathione; HMBC, long-range proton-carbon heteronuclear multiple bond correlation; IDA, information-dependent acquisition; LC-MS/MS, liquid chromatography-tandem mass spectrometry; MRM, multiple-reaction monitoring; NAC, *N*-acetyl cysteine; NADPH, β-nicotinamide adenine dinucleotide 2'-phosphate reduced tetrasodium salt; NMR, nuclear magnetic resonance; TAEA, 1,3,8-triacetylemodic acid ; TAEM, 1,3,8-triacetylemodin; TA-ω-OHEM, 1,3,8-triacetyl-ω-hydroxyemodin; THF, tetrahydrofuran.

REFERENCES

(1) Patil, S. M., Sapkale, G. N., Surwase, U. S., and Bhombe, B. T. (2010) Herbal medicines as an effective therapy in hair loss-a review. *Res. J. Pharm. Biol. Chem. Sci. 1*, 773-781.

(2) Lv, L. S., Shao, X., Wang, L. Y., Huang, D. R., Ho, C. T., and Sang, S. M. (2010) Stilbene glucoside from polygonum multiflorum thunb.: a novel natural inhibitor of advanced glycation end product formation by trapping of methylglyoxal. *J. Agric. Food Chem. 58*, 2239-2245.

(3) Lv, L. S., Gu, X. H., Tang, J., and Ho, C. T. (2007) Antioxidant activity of stilbene glycoside from Polygonum multiflorum Thunb in vivo. *Food Chemistry 104*, 1678-1681.

(4) Ryu, G., Ju, J. H., Park, Y. J. (2002) The radical scavenging effects of stilbene glucosides from Poygonum multiflorum. *Arch. Pharm. Res. 25*, 636-639.

(5) Wang, C. Y., Gu, J. M., Liu, W. N., Yang, W., and Zhang, L. T. (2009) Studies on pharmacokinetics and tissue distribution of stilbene glycoside in the hyperlipide miamodel rats. *Chinese Journal of Pharmaceutical Analysis 29*, 1073-1078.

(6) Wang, X. M., Zhao, L. B., Han, T. Z., Chen, S. F., and Wang, J. L. (2008) Protective effects of 2,3,5,40-tetrahydroxystilbene-2-O-beta-D-glucoside, an active component of Polygonum multiflorum Thunb, on experimental colitis in mice. *Eur. J. Pharmacol. 578*, 339-348.

(7) Ding, Y., Zhao, L., Mei, H., Zhang, S. L., Huang, Z. H., Duan, Y. Y., and Ye, P. (2008) Exploration of Emodin to treat alpha-naphthylisothiocyanate-induced cholestatic hepatitis via anti-inflammatory pathway. *Eur. J. Pharmacol. 590*, 377-386.

(8) Basu, S., Ghosh, A., and Hazra, B. (2005) Evaluation of the antibacterial activity of Ventilago madraspatana Gaertn, Rubia cordifolia Linn and Lantana camara Linn: isolation of emodin and physcion as active antibacterial agents. *Phytother. Res. 19*, 888-894.

(9) Koyama, J., Takeuchi, A., Morita, I., Nishino, Y., Shimizu, M., Inoue, M., and Kobayashi, N. (2009) Characterization of emodin metabolites in Raji cells by LC–APCI-MS/MS. *Bioorgan. Med. Chem. 17*, 7493-7499.

(10) Jung, K. A., Min, H. J., Yoo, S. S., Kim, H. J., Choi, S. N., Ha, C. Y., Kim, T. H., Jung, W. T., Lee, O. J., Lee, J. S. and Shim, S. G. (2011) Drug-induced liver injury: twenty five cases of acute hep atitis following ingestion of Polygonum multiflorum thumb. *Gut Liver 5*, 493-499.

(11) Valente, G., Sanges, M., Campione, S., Bellevicine, C., De Franchis, G., Sollazzo, R., Mattera, D., Cimino, L., Vecchione, R., and D'Arienzo, A. (2010) Herbal hepatotoxicity: a case of difficult interpretation. *Eur. Rev. Med. Pharmacol. Sci. 14*, 865-870.

(12) Furukawa, M., Kasajima, S., Nakamura, Y., Shouzushima, M., Nagatani, N., Takinishi, A., Taguchi, A., Fujita, M., Niimi, A., Misaka, R., and Nagahara, H. (2010) Toxic hepatitis induced by Show-Wu-Pian, a Chinese herbal preparation. *Intern. Med. 49*, 1537-1540.

(13) Sun, X. H., Sun, Y. W., Li, H., and Sun, W. (2010) Influence of main component of Heshouwu such as emodin, rhein and toluylene glycoside on hepatic cells and hepatoma carcinoma cell. *Modern Journal of Integrated Traditional Chinese and Western Medicine 11*, 1315-1319.

(14) Masuda, T., Haraikawa, K., Morooka, N., Nakano, S., and Ueno, Y. (1985) 2-Hydroxyemodin, an active metabolite of emodin in the hepatic microsomes of rats. *Mutat. Res. 149*, 327-332.

(15) Tanaka, H., Morooka, N., Haraikawa, K., and Ueno, Y. (1987) Metabolic activation of emodin in the reconstituted cytochrome P-450 system of the hepatic microsomes of rats. *Mutat. Res. 176*, 165-170.

(16) Murakami, H., Kobayashi. J., Masuda, T., Morooka, N., and Ueno, Y., (1987) ω-Hydroxyemodin, a major hepatic metabolite of emodin in various animals and its mutagenic activity. *Mutat. Res. 180*, 147-153.

(17) Mueller S. O., Stopper, H., and Dekant, W. (1998) Biotransformation of the anthraquinones emodin and chrysophanol by cytochrome P450 enzymes: bioactivation to genotoxic metabolites. *Drug Metab. Dispos. 26*, 540-546.

(18) Lin, D. J., Li, C. Y., Peng, Y., Gao, H. Y., and Zheng, J. (2014) Cytochrome p450-mediated metabolic activation of diosbulbin B. *Drug Metab. Dispos. 42*, 1727-1736.

(19) Banks, H. J., Cameron, D. W., and Raverty, W. D. (1978) Hydroxylation of anthraquinones in oleum and in sulfuric acid. *Aust. J. Chem. 31*, 2271-2282.

(20) Morooka, N., Itoi, N., and Ueno, Y. (1986) Identification and mutagenicity of the metabolites of emodin in hepatic microsomes of rats. *Ann. Meet. Jpn. Soc. Agric. Chem., Abstract p. 409.*

(21) Rodrigues, A. D. (1999) Integrated cytochrome P450 reaction phenotyping: attempting to bridge the gap between cDNA-expressed cytochromes P450 and native human liver microsomes. *Biochem. Pharmacol. 57*, 465-480.

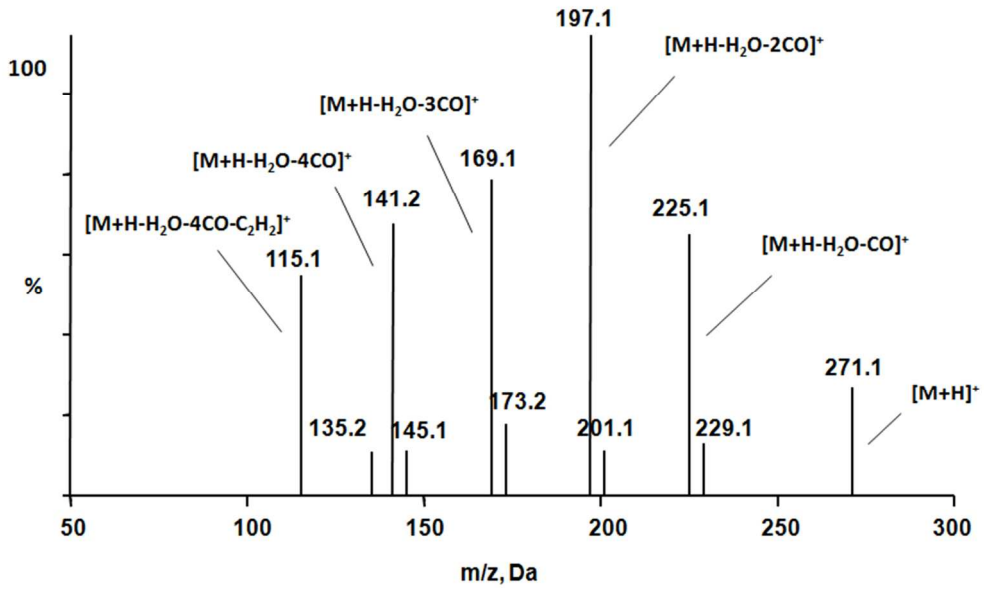

Figure 1. MS/MS spectrum of EM.

221x130mm (300 x 300 DPI)

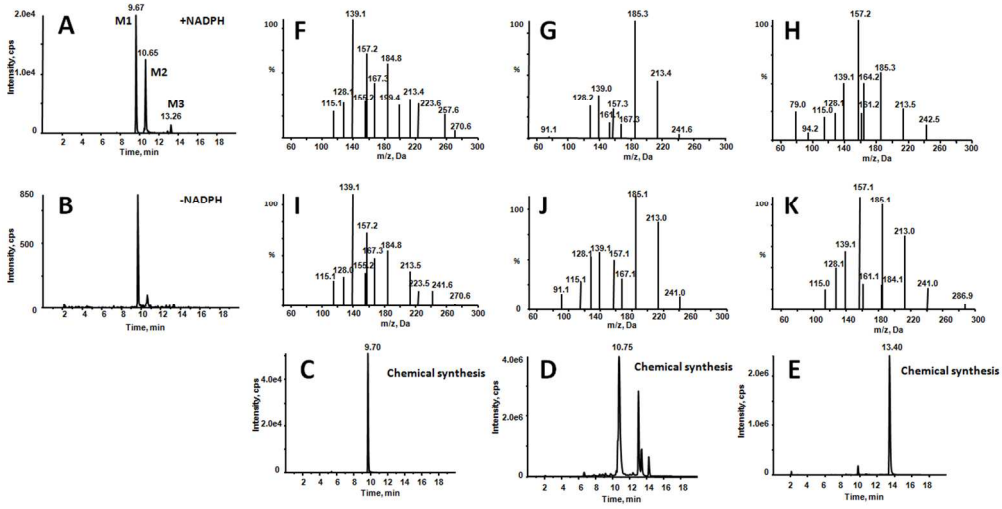

Figure 2. Identification of metabolites M1, M2, and M3. Extracted ion (m/z 287→139 for M1, M2 and M3) chromatograms obtained from LC-Q-Trap MS analysis of human liver microsomal incubations containing EM in the presence (A) or absence (B) of NADPH. Extracted ion (m/z 287→139) chromatograms obtained from LC-Q-Trap/MS analysis of synthetic M1 (C), M2 (D), and M3 (E). MS/MS spectra of M1 (F), M2 (G), and M3 (H) generated in microsomal incubations. MS/MS spectra of synthetic M1 (I), M2 (J), and M3 (K).

342x175mm (300 x 300 DPI)

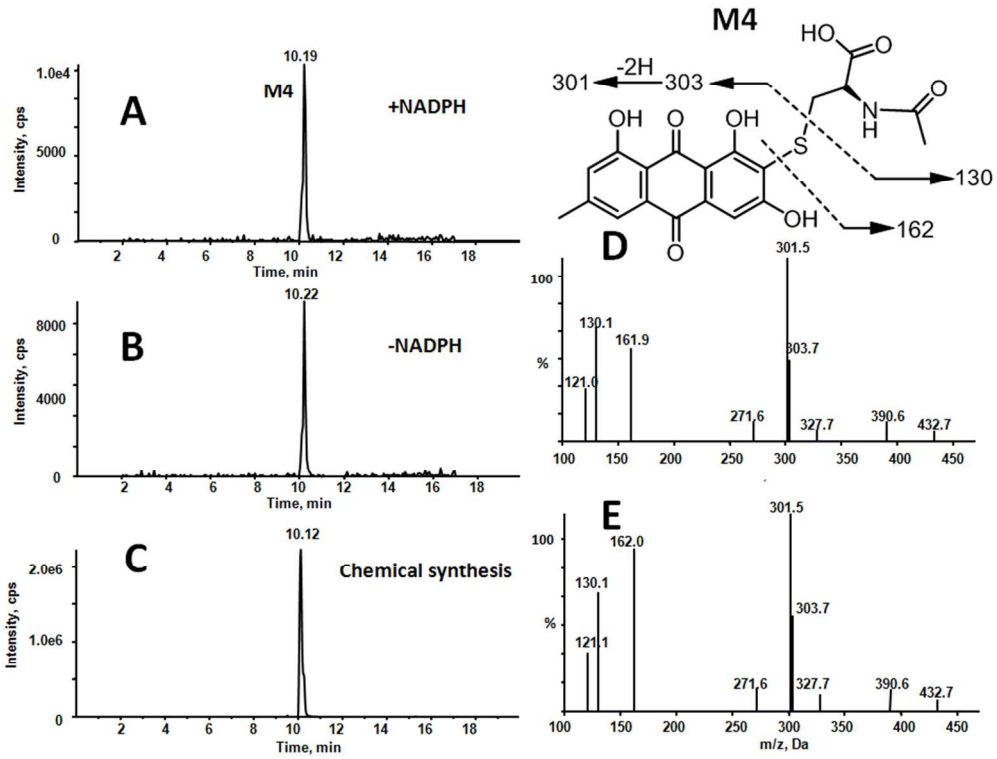

Figure 3. Identification of metabolites M4. Extracted ion (m/z 432→301 for M4) chromatograms obtained from LC-Q-Trap MS analysis of human liver microsomal incubations EM and NAC in the presence (A) or absence (B) of NADPH. (C) Extracted ion (m/z 432→301) chromatogram obtained from LC-Q-Trap MS analysis of synthetic M4. (D) MS/MS spectrum of M4 generated in microsomal incubations. (E) MS/MS spectrum of synthetic M4.

250x192mm (300 x 300 DPI)

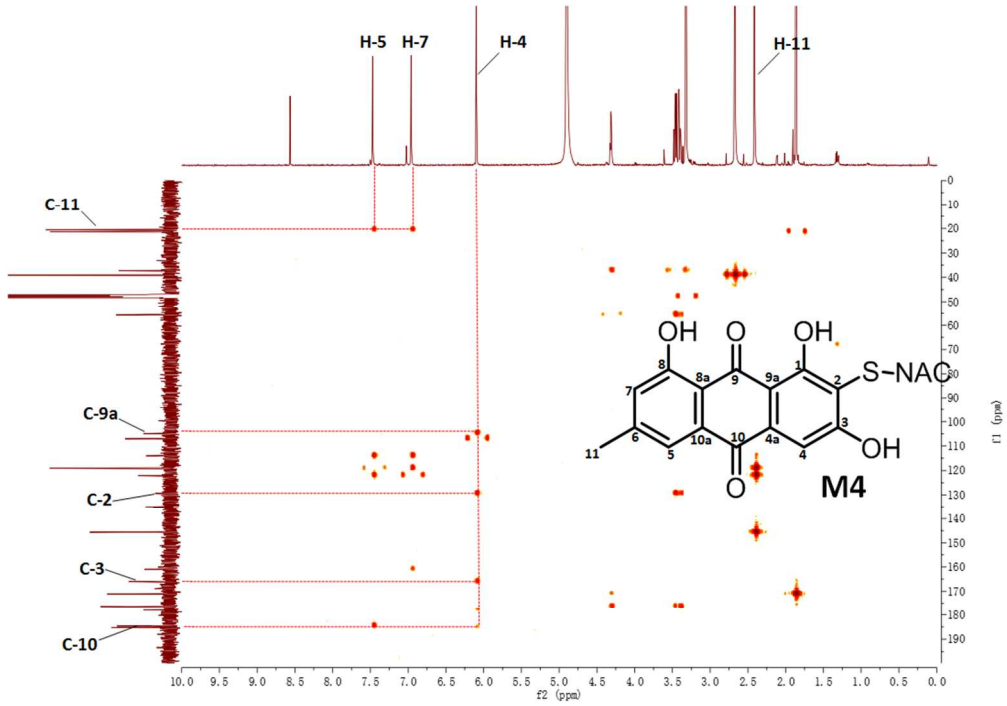

Figure 4. HMBC (long-range proton-carbon heteronuclear multiple bond correlation) spectra of M4.

289x203mm (300 x 300 DPI)

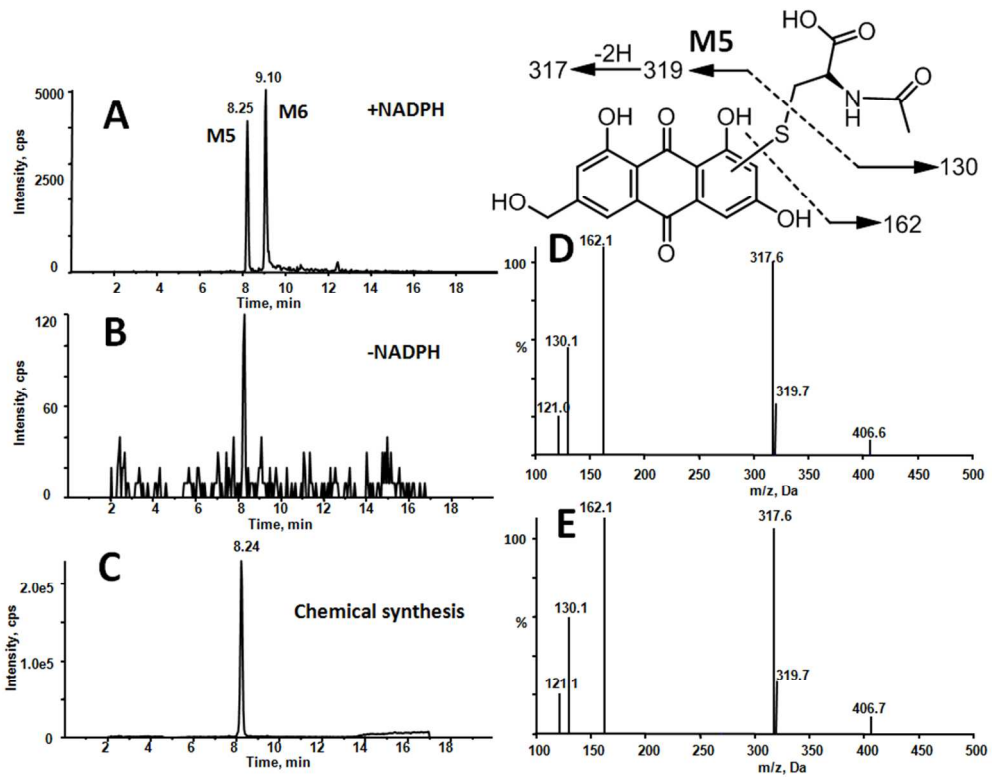

Figure 5. Identification of metabolites M5. Extracted ion (m/z 448→317 for M5) chromatograms obtained from LC-Q-Trap MS analysis of human liver microsomal incubations EM and NAC in the presence (A) or absence (B) of NADPH. (C) Extracted ion (m/z 448→317) chromatogram obtained from LC-Q-Trap MS analysis of synthetic M5. (D) MS/MS spectrum of M5 generated in microsomal incubations. (E) MS/MS spectrum of synthetic M5.

253x195mm (300 x 300 DPI)

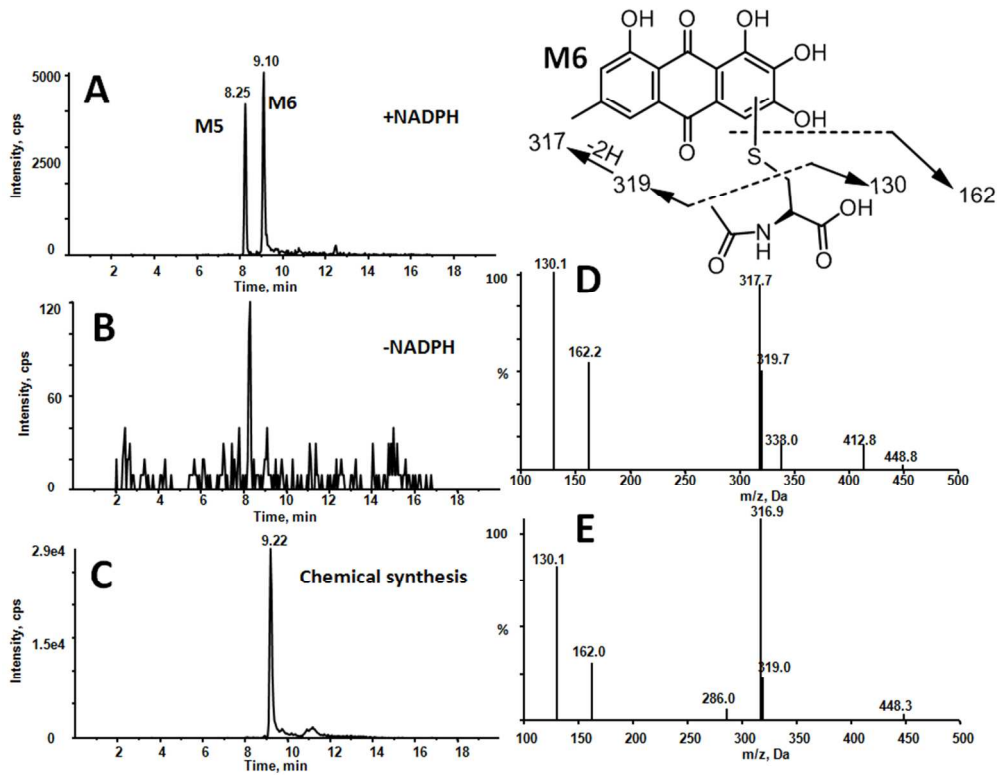

Figure 6. Identification of metabolites M6. Extracted ion (m/z 448→317 for M6) chromatograms obtained from LC-Q-Trap MS analysis of human liver microsomal incubations EM and NAC in the presence (A) or absence (B) of NADPH. (C) Extracted ion (m/z 448→317) chromatogram obtained from LC-Q-Trap MS analysis of synthetic M6. (D) MS/MS spectrum of M6 generated in microsomal incubations. (E) MS/MS spectrum of synthetic M6.

256x197mm (300 x 300 DPI)

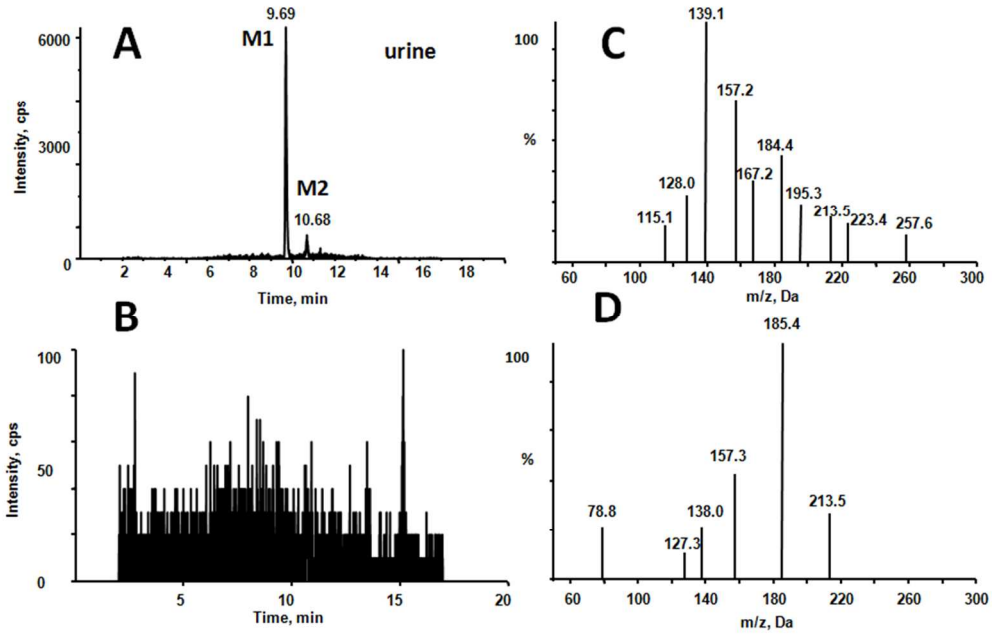

Figure 7. Extracted ion (m/z 287→139 for M1 and M2) chromatograms obtained from LC-Q-Trap MS analysis of the urine of rats after (A) and before (B) treatment with EM. MS/MS spectra of M1 (C) and M2 (D) in the urine samples of rats administered with EM.

231x148mm (300 x 300 DPI)

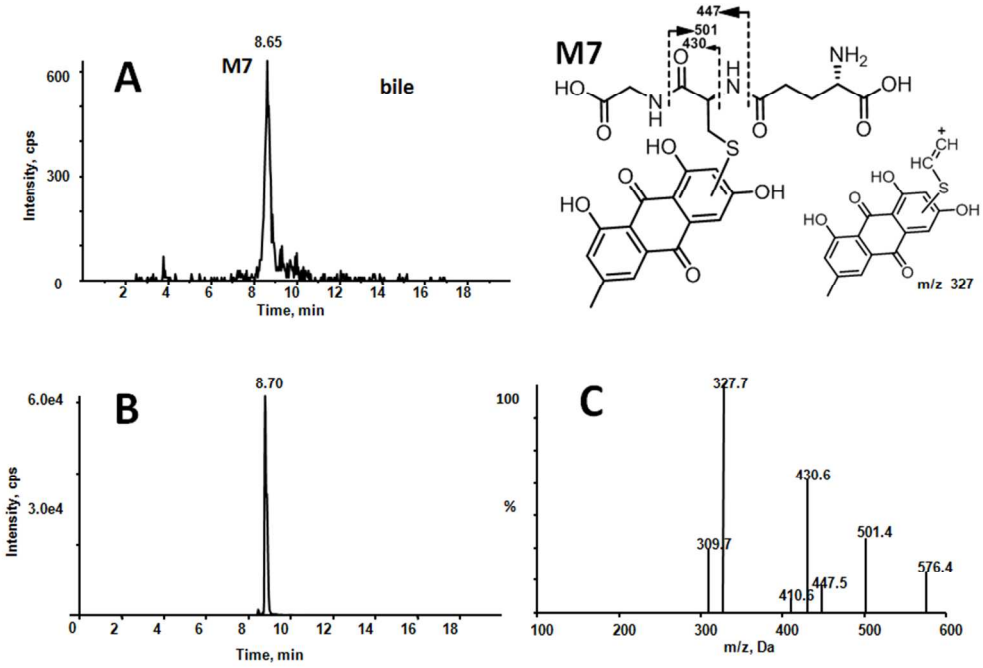

Figure 8. Extracted ion (m/z 576→327 for M7) chromatograms obtained from LC-Q-Trap MS analysis of bile (A) from rats given EM. Extracted ion (m/z 576→327 for M7) chromatograms obtained from LC-Q-Trap MS analysis of rat liver microsomal incubations EM and GSH in the absence (B) of NADPH. MS/MS spectra of M7 (C) in the bile samples of rats administered with EM.

240x160mm (300 x 300 DPI)

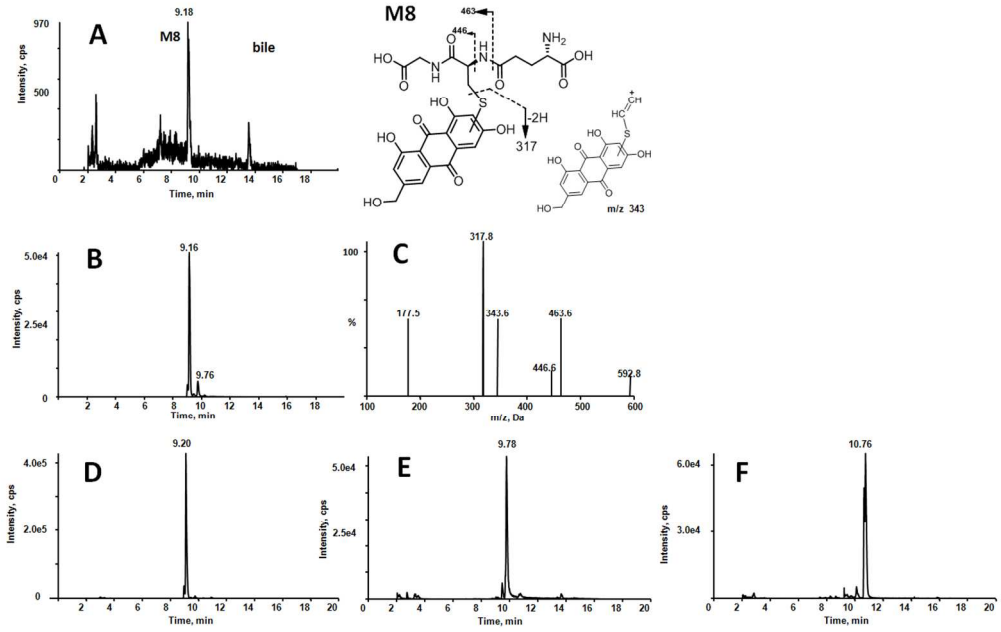

Figure 9. Extracted ion (m/z 592→463 for M8) chromatograms obtained from LC-Q-Trap MS analysis of bile (A) from rats given EM. Extracted ion (m/z 592→463 for M8) chromatograms obtained from LC-Q-Trap MS analysis of rat liver microsomal incubations EM and GSH in the presence (B) of NADPH. MS/MS spectra of M8 (C) in the bile samples of rats administered with EM. Extracted ion (m/z 592→463) chromatograms obtained from LC-Q-Trap/MS analysis of synthetic GSH conjugates derived from ω-hydroxyemodin (D), 2-hydroxyemodin (E), and 5-hydroxyemodin (F).

365x231mm (300 x 300 DPI)

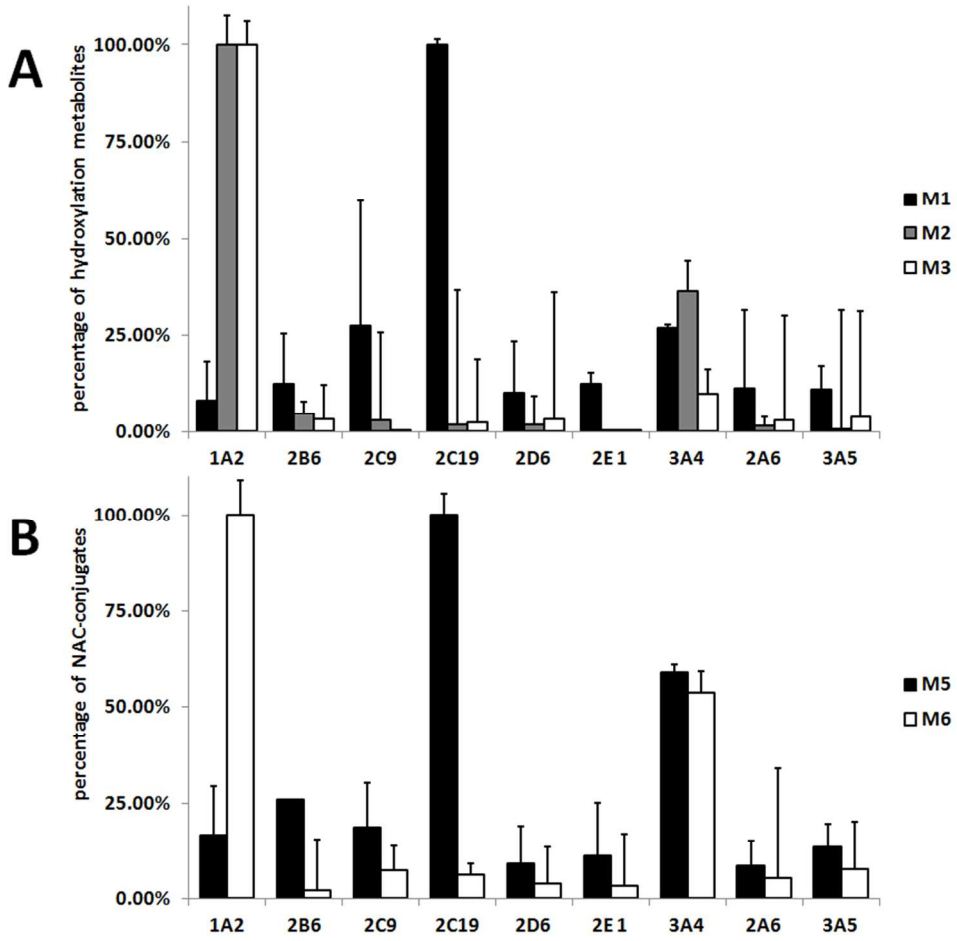

Figure 10. Individual human recombinant P450 enzymes involved in bioactivation of EM. EM was incubated with individual human recombinant P450 isoforms and NADPH in the absence (A) or presence (B) of NAC. The catalytic capabilities of the enzymes were evaluated by monitoring the formation of M1-M3 and M5-M6 after normalization based on the relative content of the corresponding P450 enzyme in human liver microsomes. Data represent the mean ± S.D. (n = 3).

238x229mm (300 x 300 DPI)

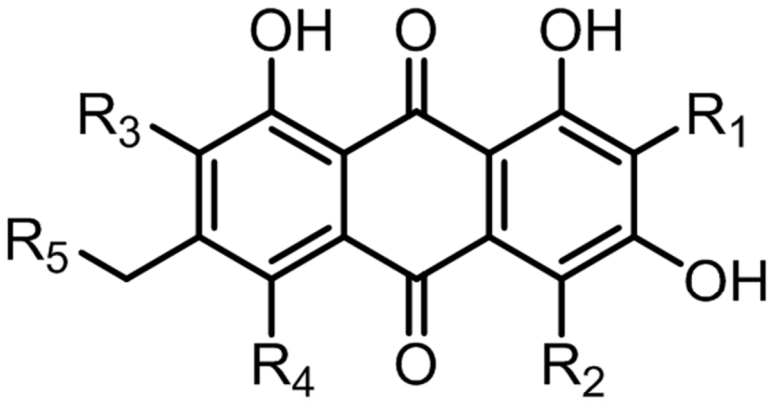

compounds	R_1	R_2	R_3	R_4	R_5
EM	H	H	H	H	H
2-hydroxyemodin	OH	H	H	H	H
4-hydroxyemodin	H	OH	H	H	H
7-hydroxyemodin	H	H	OH	H	H
5-hydroxyemodin	H	H	H	OH	H
ω-hydroxyemodin	H	H	H	H	OH

Scheme 1.

193x194mm (300 x 300 DPI)

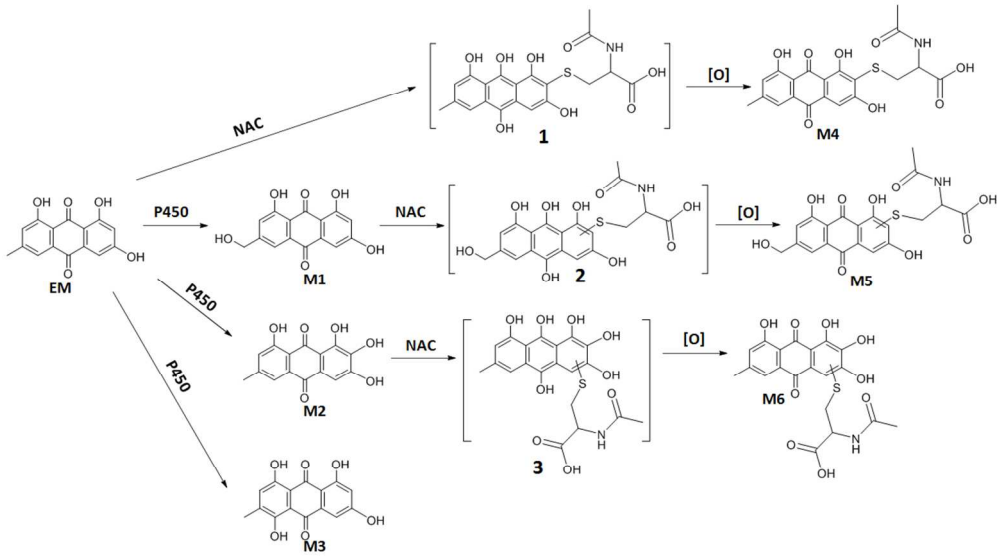

Scheme 2. Proposed pathways for the formation of EM metabolites mediated by cytochromes P450

106x59mm (300 x 300 DPI)

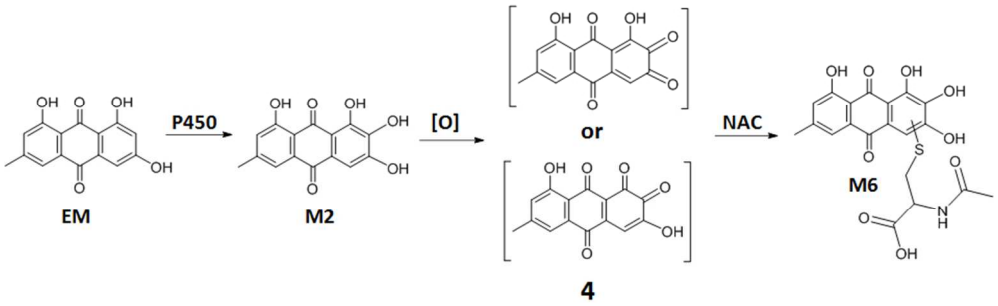

Scheme 3. Another proposed pathway for the formation of M6 mediated by cytochromes P450

81x25mm (300 x 300 DPI)